Geophysical Journal International

Geophys. J. Int. (2025) **241,** 728–742
Advance Access publication 2025 February 19
GJI Seismology

https://doi.org/10.1093/gji/ggaf068

Relocating seismic events in the North Sea: challenges and insights for earthquake analysis

Annie Elisabeth Jerkins [1,2], Johannes Schweitzer [1,2], Tom Kettlety [3], Evgeniia Martuganova [4], Daniela Kühn [1,5] and Volker Oye [1,6]

[1] *NORSAR, Gunnar Randers vei* 15, 2027 *Kjeller, Norway. E-mail: annie@norsar.no*
[2] *PHAB, University of Oslo,* 0371 *Oslo, Norway*
[3] *Department of Earth Sciences, University of Oxford, S Parks Rd, Oxford OX*13*AN, Great Britain*
[4] *Faculty of Civil Engineering and Geosciences, Delft University of Technology, Stevinweg* 12628 *CN Delft,* 5048 2600 *GA Delft, The Netherlands*
[5] *GFZ German Research Centre for Geosciences, Wissenschaftpark 'Albert Einstein', Telegrafenberg,* 14473 *Potsdam, Germany*
[6] *Department of Geoscience, University of Oslo,* 0371 *Oslo, Norway*

Accepted 2025 February 17. Received 2025 January 21; in original form 2024 October 29

SUMMARY

In this paper, we present a catalogue of relocated seismic events in the North Sea spanning 1961 to 2022. Data from all relevant agencies were combined, incorporating all available seismic phase readings, thereby enhancing station coverage. As a result, our updated locations reveal a more clustered and aligned seismicity pattern compared with the original catalogue. Even with our combined data set, only 157 of the 7089 relocated events have azimuthal gaps of less than 90 deg. Additionally, the distances between onshore stations and offshore events are considerable. Both of these factors lead to relatively poorly constrained hypocentres for most events. We therefore evaluate the performance of 1-D velocity models routinely used by different North Sea adjacent monitoring agencies for earthquake location estimations in the North Sea. The variations in assessments due to the seismic velocity model used are significantly larger than the uncertainty ellipses calculated in the relocation, demonstrating that arithmetic uncertainties systematically underestimate location uncertainties in this setting. Obtaining a realistic estimate of location uncertainty is however crucial, particularly for distinguishing between natural and induced seismicity. This is fundamental to safe monitoring of the North Sea offshore industries, including geological CO_2 storage. To overcome these discrepancies between the uncertainty ellipses and our multiple relocations, we introduce an alternative method that accounts for variability in the 1-D velocity models. This approach enhances the reliability of the earthquake catalogue, and provides a more robust assessment of seismic activity in the North Sea.

Key words: Europe; Spatial analysis; Earthquake parametrization; Earthquake source observations; Seismicity and tectonics.

1 INTRODUCTION

The International Energy Agency and the Intergovernmental Panel on Climate Change stated that carbon capture and storage (CCS) is essential to reduce the effects of greenhouse gas emissions (Heidug 2013; IPCC 2023). Due to its geology, existing infrastructure, and technical expertize from oil and gas operations (Furre *et al.* 2019; Jerkins *et al.* 2023), the North Sea is particularly suited for geologic CO_2 storage. A notable CCS project is the Northern Lights initiative, led by the Northern Lights joint venture (comprising of Equinor, Shell, and Total Energies). Their aim is to launch a full-scale CCS project southwest of the Troll field on the Horda platform in 2024 (Furre *et al.* 2020) (see Fig. 1). Several CO_2 storage licensing rounds have also recently concluded for the UK offshore territory, with dozens of licences awarded (North Sea Transition Authority 2024). High profile projects such as Endurance in the UK offshore area, Porthos and Aramis offshore of the Netherlands, and Greensands offshore of Denmark, all plan for large scale CO_2 injection before 2030.

For the long-term success of CCS, the understanding of the natural background seismicity is crucial (Zarifi *et al.* 2023). Such knowledge helps to avoid CO_2 injection in earthquake-prone areas,

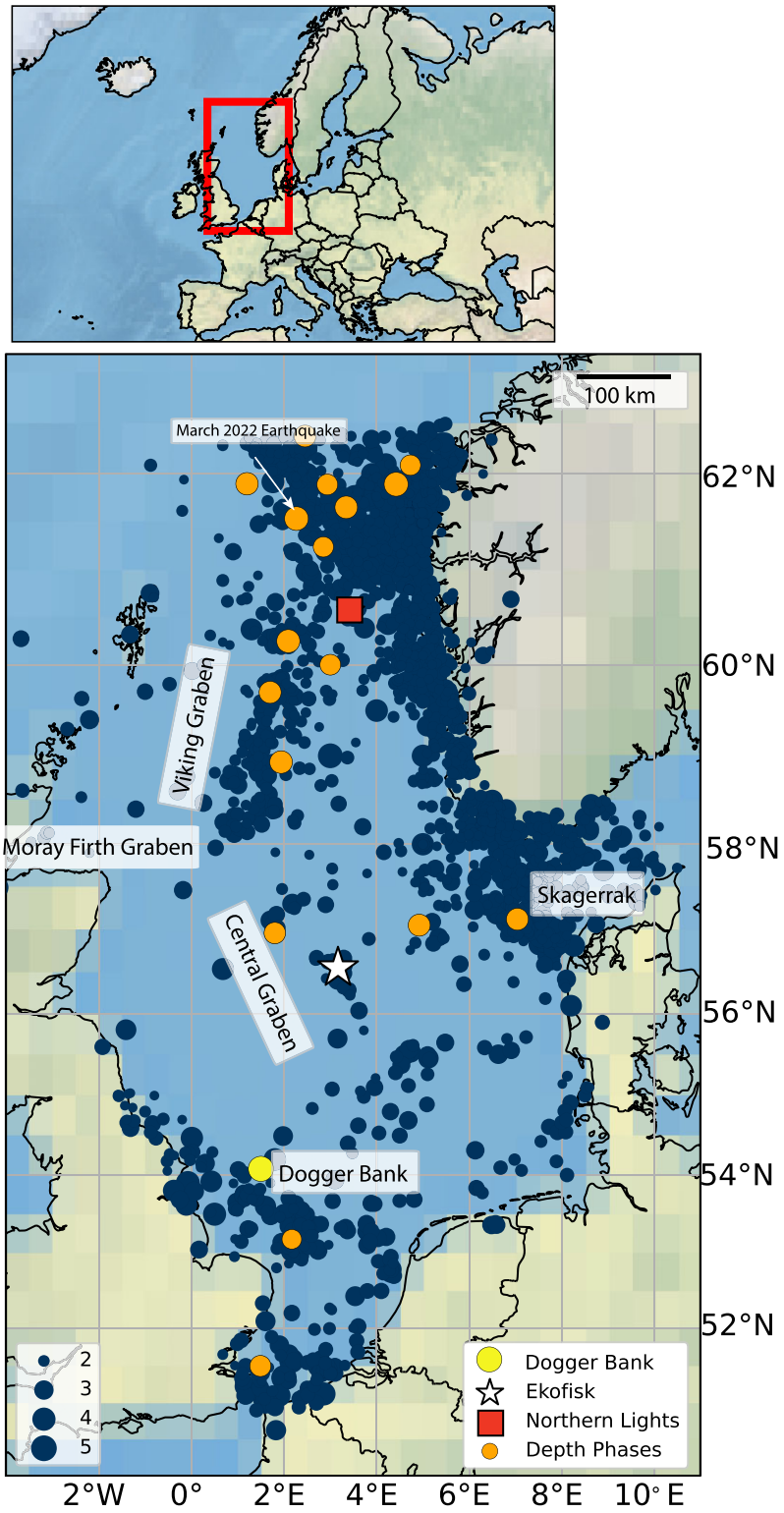

Figure 1. Locations of seismic events within the North Sea region with reported magnitudes above 2 from the SHARP catalogue (magnitudes represented by circle sizes). 17 events with observed depth phases are highlighted in orange. The Ekofisk earthquake is denoted by a white star, while a red rectangle indicates the Northern Lights CO_2 storage site. A yellow dot near the 'Dogger Bank' label marks the M_w 5.3 event from 1931.

to detect abnormal seismic events potentially linked to injection and to evaluate the risk to the storage complex (Cappa & Rutqvist 2011).

While the level of seismicity in the North Sea is typically considered low to intermediate (e.g. Bungum *et al.* 1991), the frequency and magnitudes of seismic events are sufficiently large to be taken into account when constructing offshore installations (Hansen *et al.* 1989). For instance, several earthquakes with magnitude 4 or larger have occurred across the North Sea region. The most recent was the M_w 5.1 Tampen Spur earthquake in 2022 March in the Northern North Sea (Zarifi *et al.* 2023; Jerkins *et al.* 2024). As this

earthquake occurred only a few kilometers from the Snorre oil field, it caused a temporary shutdown of the Snorre B platform. The largest instrumentally recorded seismic event up to date in the region is the M_w 5.3 event in the Dogger Bank area on 1931 June 7 (Bungum *et al.* 2003). There are clear concentrations in the seismicity pattern, where the earthquake density is most pronounced: just offshore Norway, in the Viking Graben gradually decreasing towards the central Graben, in the Skagerak (between southern Norway and Denmark), and along the southeast coast of the United Kingdom in the Dogger Bank region (Bungum *et al.* 1991); see Fig. 1.

Causes of earthquake occurrence in the North Sea are complex. The North Sea has undergone two rifting stages evident by three Graben structures: the Viking, Central and Moray Firth Graben. These structures interconnect forming a triple junction. The initial formation of the basin framework can be traced to the Early Paleozoic era (Bartholomew *et al.* 1993). Rifting activity continued into the early Triassic and crustal extension happened during the Late Jurassic to Early Cretaceous (Talwani & Eldholm 1977). The incomplete rifting resulted in the creation of multiple faults and fracture systems. These planes of weakness can be reactivated by earthquakes due to the build up of tectonic stress over time. Studies suggest that this stress originates either from ridge-push forces at the Mid-Atlantic ridge or from isostatic rebound after the last glaciation (Bungum *et al.* 2005; Jerkins *et al.* 2020).

Additionally, a few earthquakes in the North Sea were induced by human activities associated with oil and gas production. For example, on 2001 May 7, an Mw 4.3 earthquake was caused by water injection in the overburden of the Ekofisk field (Ottemöller *et al.* 2005; Selby *et al.* 2005; Cesca *et al.* 2011); indicated by a white star in Fig. 1.

Any subsurface project carries the risk of induced or triggered seismicity. Commonly, determining whether a small-magnitude earthquake is natural or induced/triggered depends on the location of the earthquake (Garcia-Aristizabal *et al.* 2020), but also other factors such as its source parameters, underlying physics or - for sequences - statistics (Dahm *et al.* 2013). Cheng *et al.* (2023) reviewed potential mechanisms for induced seismicity related to CCS. They highlighted the significant challenges in identifying fault systems and the complexities in assessing the likelihood of their reactivation. Studying detailed properties of seismic events is therefore essential. Additionally, accurately reporting and acknowledging uncertainties in earthquake locations is important for oil and gas authorities as well as for public acceptance of CCS projects.

The work conducted here was a part of an Accelerating CCS technology project SHARP Storage (Stress History And Reservoir Pressure for improved quantification of CO_2 storage containment risks). The objective of SHARP was to improve the quality of subsurface CO_2 storage containment risk management by evaluating geological stress models, seismicity observations and rock mechanical failure.

As a part of the SHARP project, earthquake catalogues were collected from the International Seismological Center (ISC) (Di Giacomo *et al.* 2018; International Seismological Centre 2024) as well as from local agencies in Germany, the Netherlands, the UK, Norway, and Denmark to create a uniform catalogue of seismic events in the North Sea consisting of over 12 000 seismic events (for details see Kettlety *et al.* (2024)). The locations of events with an average magnitude (average of all reported magnitudes) above 2 are shown in Fig. 1.

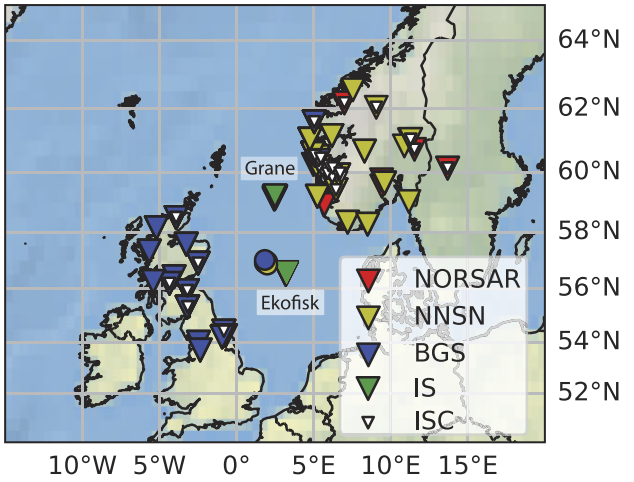

Figure 2. Improved azimuthal coverage for an M_L 2.7 event on 2021 February 14 at 09:04 GMT; circles represent event locations, triangles denote stations, both coloured according to the agency reporting the phase pick. The industry sensors stem from permanent reservoir systems at Ekofisk and Grane operated by ConocoPhillips and Equinor, respectively (data from selected sensors are continuously sent to NNSN).

It is essential to note that the neighbouring seismological agencies employ different methods and velocity models for their routine analyses of events in the North Sea. Merging catalogues provides a higher number of phase readings and reduces azimuthal gaps, which is expected to enhance the quality of the derived locations. An example of how the station coverage is improved for a seismic event in the central part of the North Sea is shown in Fig. 2. For this event, combining phase readings from multiple sources, NORSAR (1971), Norwegian National Seismic Network (1982) (NNSN), British Geological Survey (1970) and International Seismological Centre (2024), clearly improve its azimuthal coverage. Note that the agencies partially share data with each other, usually on a bilateral basis. For instance, NORSAR contributes to the NNSN bulletin and both are reporting to the ISC. This leads to duplicates in the catalogue. In our visualization, we only show the initial agency mentioned for each phase reading.

This study presents event relocations for the newly compiled catalogue of North Sea seismic events (Kettlety *et al.* 2024). First, we provide a brief description of the workflow in compiling this catalogue, supplemented with statistical information providing further insights (see Kettlety *et al.* 2024 for a detailed description). We then show an overview of the seismic stations whose records contribute to the catalogue and the available velocity models. This is followed by a description of the method employed for relocation, with an emphasis on testing multiple 1-D velocity models and discussing the associated uncertainties.

The relocation process is conducted with a methodology further developed from Schweitzer *et al.* (2021), who relocated a 24-year-long seismic bulletin for the European Arctic. The seismological agencies aim to lower the magnitude of completeness in their catalogues, which is especially important for hazard and risk studies. However, earthquakes recorded on a limited number of stations often result in poorly constrained hypocentre estimates. This lack of accuracy disturbs the general trends of the seismicity pattern, limiting the understanding of faulting in the region. To address this issue, we apply specific quality criteria to ensure that only high-quality locations are included in the final bulletin. Finally, we provide a statistical analysis of relocation results, highlighting our key findings.

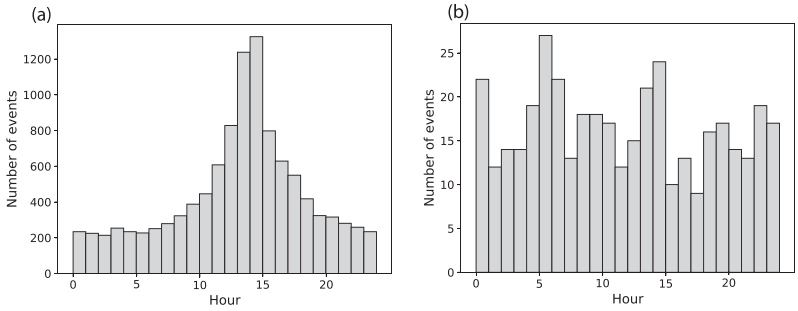

Figure 3. Time-of-day distribution of seismic events. In panel (a), we present events below magnitude 3, and in panel (b), we display events above magnitude 3.

We conclude with a discussion, presenting strategies for improving earthquake locations further for offshore CO_2 storage monitoring.

2 EVENT CATALOGUE AND STATISTICS

For a detailed description of the initial catalogue and its creation, see Kettlety *et al.* (2024). The catalogue was created by defining a polygon covering the entirety of the North Sea region. Seismic events were collected from the following agencies: International Seismological Centre (2024), Royal Observatory of Belgium (1985), Geological Survey of Denmark and Greenland (2023), German Research Centre for Geosciences (1993), Federal Institute for Geosciences and Natural Resources (1976), Royal Netherlands Meteorological Institute (1993), NORSAR (1971), Norwegian National Seismic Network (1982), British Geological Survey (1970), Christian Albrechts - Universitat zu Kiel (2017) and from the MAGNUS temporary deployment (Weidle *et al.* 2010).

Efforts were made to refine and clean the catalogue. Multiple methods were applied to detect duplicates and erroneous events. Events with similar origin times were merged into one entry, likewise phase arrivals with similar phase pick onset times. Each onset time and origin entity was assigned a unique identity code.

In a second step, we defined 'prime' locations for each event, which will be referred to in the following as original locations (as shown in Fig. 1). These were determined by first calculating the circular mean of all origins given by agencies, and subsequently selecting the origin closest to the circular mean.

Furthermore, explosions were identified and removed as far as possible. To correctly characterize seismicity, agencies typically label explosions or suspected explosions by using available reports from military and roadwork authorities, checking locations such as quarries or mining sites, or analysing waveforms, frequency content, and infrasound signals. In Fig. 3, we present a distribution of events in the catalogue according to the time of day. Notably, the majority of seismic events with average magnitudes below 3 were registered during working hours (the average magnitude is estimated by calculating the mean of all reported magnitudes). Meanwhile, for events above average magnitude 3, the distribution is more balanced. This observation suggests that a considerable number of explosions remained in the catalogue. Given that there are 10 883 events with magnitudes below 3 and an hourly average of 200 registered events during the night, we estimate the presence of roughly 6000 explosions, comprising nearly half of the events in the current catalogue. However, we do not remove these potential explosions, to avoid the risk of removing potential earthquakes.

Fig. 4(a) presents the temporal distribution of the catalogued seismic events. Prior to the 1960s, the limited station coverage had the consequence that only larger seismic events were recorded. We note that the first seismic event located in this study occurred in 1961. As the network of stations expanded, more seismic events were detected and reported. The fluctuations in the number of recorded events after the 1980s may be attributed to temporary station deployments, changes in personnel analysing the data, modifications in detection procedures, or simply increased seismic activity in certain years.

In Fig. 4(b), we show the number of events versus local magnitude (since M_L was also reported by Kettlety *et al.* (2024), and it is the most frequently reported magnitude type in the catalogue). The detection threshold limits the number of small events, and we do not detect many events below magnitude 1. Most events are in the range between magnitudes 1 and 2, and the number of larger events is strictly limited, with only a few events exceeding magnitude 4. Naturally, this detection capability varies significantly in space across the North Sea. The earliest events in the data set date back to the 14th century and come from British Geological Survey (BGS) records of historical seismicity, which are included in their seismicity catalogue. Naturally, without any phase information, these are not relevant to this study. The spatiotemporal variations in the magnitude of completeness could not thoroughly be evaluated in Kettlety *et al.* (2024). Based on the magnitude–frequency distributions of the full data set, they determined a practical completeness of magnitude 4 since around 1980 in the region.

Fig. 4(c) illustrates the annual number of distinct stations listed per year since 1960. As shown in Fig. 4(c), the initial number of seismic stations was sparse. Over the years, the number seismic stations has gradually increased. However, we note that in certain years—specifically 1989, 2017 and 2022—there are pronounced peaks compared to the more typical years. These peaks are caused by larger magnitude seismic events (greater than M_w 4.5), which were also recorded by sensors at teleseismic distances, resulting in a significant increase in the number of distinct stations listed for those years.

An overview of the number of stations listed for each seismic event in the catalogue is provided in Fig. 4(d). Seismic events not recorded on any station are identified by macroseismic observations only.

A key challenge in locating seismic events in the North Sea is the limited resolution of hypocentre depths, which is largely due to the extensive event-station distances. One approach to improve the depth estimate for larger seismic events is to employ teleseismic depth phases (e.g. Engdahl *et al.* 1998). However, within the catalogue, only 17 events were reported with observed pP or sP phases

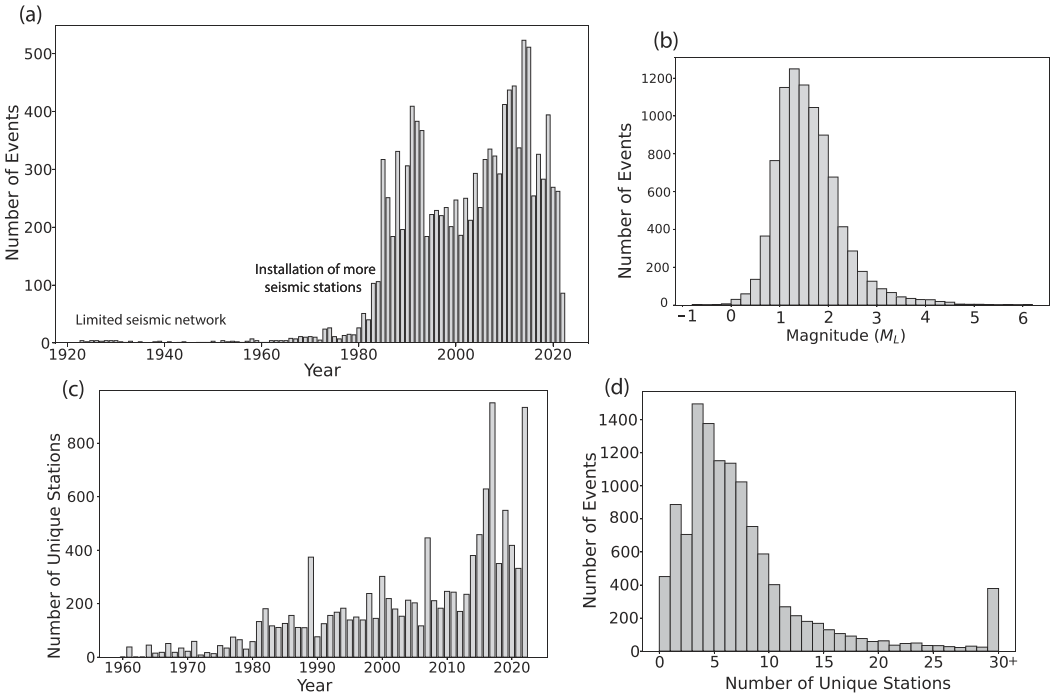

Figure 4. Distribution of seismic events over time in the catalogue. (a) Annual number of events registered from the 1920s to 2022. Note that the catalogue was compiled up to 2022 July, resulting in fewer events recorded for that year. (b) Histogram showing the number of events per local magnitude. (c) Annual number of distinct stations per year included in the catalogue. (d) Number of stations reporting each seismic event.

(Fig. 1). This means that depth resolution remains a challenge, with event depths either left unconstrained or fixed, depending on the practices of the reporting agencies.

2.1 Stations in catalogue

The catalogue comprises events recorded on 2620 unique seismic stations, for which we collected as many of the coordinates as possible. First, an initial search was performed using the station list provided by International Seismograph Station Registry (2024). Subsequently, we conducted searches within station files provided by local and regional agencies of the North Sea bordering states.

Especially within the United States and Europe, the station density is high. Stations in the United States were mostly used for teleseismic depth phase readings for larger earthquakes. Stations surrounding the North Sea are featured in Fig. 5 highlighting available phase readings reported in the catalogue. Stations further from the North sea generally record fewer events in this North Sea catalogue. A large amount of phase readings were derived from stations along Norway's west coast, especially from station ASK (21 053 phase readings in total).

2.2 Velocity models

The seismological agencies employ various velocity models for routine analysis of earthquakes in the North Sea. These models are illustrated in Fig. 6 and together with the affiliated agencies detailed in Table 1. We note that all agencies use Vp/Vs ratios in the range between 1.68 and 1.79 to derive their *S*-wave velocity models. As a part of the SHARP project, a new model was developed by averaging CRUST1.0 models (Laske *et al.* 2013) for the North Sea.

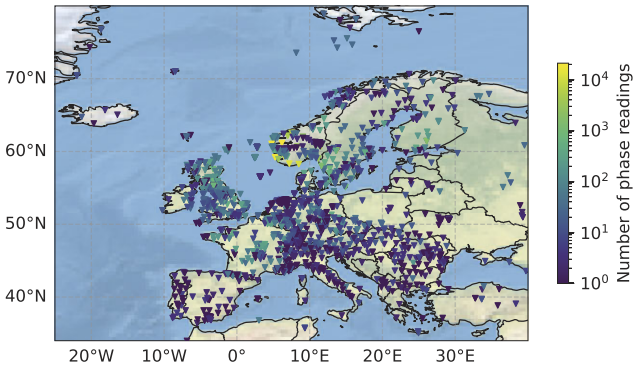

Figure 5. Stations used to locate the catalogued seismic events distribution within Europe (1401 stations). The number of available phase readings is indicated by the logarithmic colour scale.

In this SHARP model, the Vp/Vs ratio varies from 3.1 in the upper layer to 1.71 at the Moho.

These models show significant discrepancies, especially within the shallow layers. Notably, the models called North Netherlands, South Netherlands, SHARP, and BGS Dover have considerably slower velocities in the uppermost crust. These differences arise from the varying geological conditions of the countries surrounding the North Sea. For instance, in the Netherlands and Denmark, most seismic stations are placed atop soft sediments, while in Norway, stations are most often positioned directly on bedrock. Therefore, the use of a 3-D velocity model encompassing the entire region would be optimal to account for the significant geological variations across the area. However, such a model is currently not available and its creation is beyond the scope of this work.

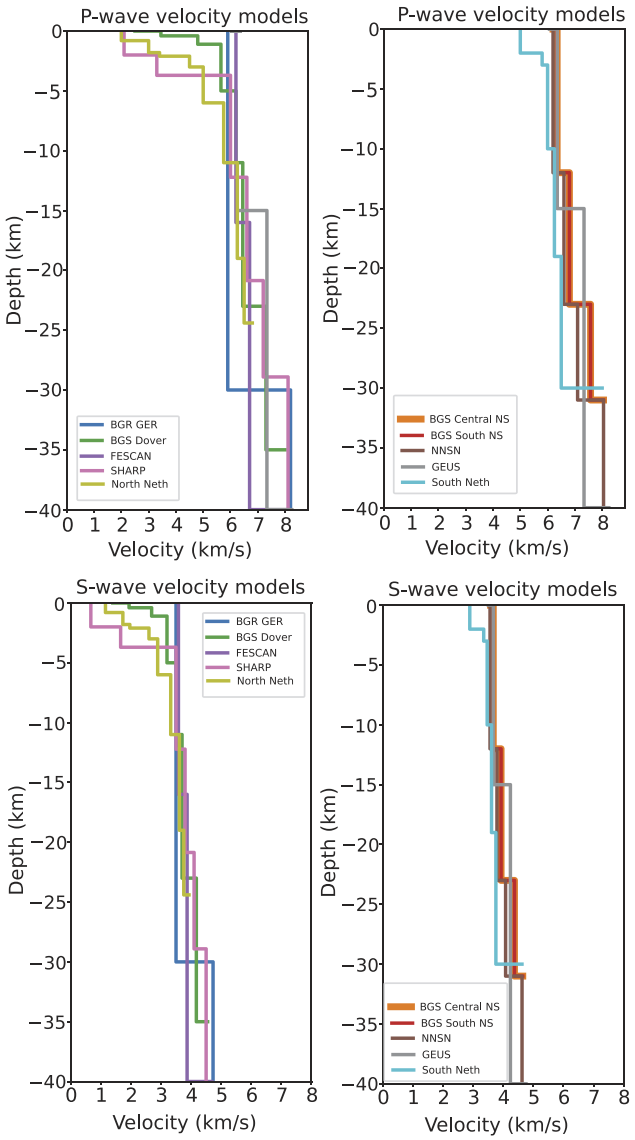

Figure 6. Velocity models employed for relocating earthquakes used by various seismological agencies of countries surrounding the North Sea.

Table 1. Velocity models and corresponding countries/agencies. [1]Mykkeltveit & Ringdal (1981), [2]Havskov & Bungum (1987), [3]Laske *et al.* (2013).

Velocity model	Agency, country
BGR-GER	BGR, Germany
BGS Central North Sea	BGS, UK
BGS Dover Strait	BGS, UK
BGS South North Sea	BGS, UK
FESCAN	NORSAR, Norway[1]
NNSN	NNSN, Norway[2]
SHARP	CRUST1.0 average[3]
GEUS	GEUS, Denmark
North Neth	KNMI, Netherlands
South Neth	KNMI, Netherlands

3 EARTHQUAKE RELOCATION

For earthquake relocation, we apply the HYPOSAT location algorithm by Schweitzer (2001), which is further detailed in Schweitzer (2018). This algorithm is based on a generalized matrix inversion and allows the inclusion of a large variety of input parameters, such as backazimuths, onset times, and traveltime differences. In this process, each event is considered individually, employing a single-event rather than a multiple-event relocation method. It is important to note that we employ phase picks from the existing catalogue and do not re-pick or perform any additional waveform analysis.

To ensure the quality of the relocations, we employ several selection criteria for the data and earthquakes considered. Magnitude estimates were disregarded initially due to variability in measurement methods among different agencies, though magnitudes will be re-estimated at a later stage. For now, we use the average of the reported magnitudes. Certain data types, such as T-phase readings, long-period surface waves, and infrasound readings, were excluded due to their inherent significant uncertainties.

We include *P*- and *S*-wave arrivals and utilize S-P times where available. Backazimuth and slowness measurements from seismic arrays were also used. Phases labelled 'x' in the bulletin underwent manual verification for potential relabelling or exclusion from the final solution. In this context 'x' is an unidentified arrival (Storchak *et al.* 2003). These 'x'-labelled phases constitute 3.7 per cent of the total number of phases in the data set.

Only events registered on more than five stations were relocated, in order to ensure better-constrained locations, leading to 7089 relocated seismic events. We assumed the following general uncertainties for phase readings (these are the same as those from Schweitzer *et al.* 2021): 0.5 s for *P*-wave readings and 0.87 s for *S*-wave readings. Station elevation corrections were applied based on phase type, using crustal velocities of 5.8 km s^{-1} for *P*-wave arrivals and 3.46 km s^{-1} for *S*-wave arrivals. Only stations within a 10-deg radius of the events were considered to obtain robust relocation, and to avoid including information from too distant stations that may bias the solutions. We note, however, that regional phases have less well-understood traveltimes due to crustal and upper mantle complexities compared to phases from greater distances. Nonetheless, most events are recorded only on local and regional networks.

Phases with residuals larger than 4 s were disregarded; these phases were manually checked after relocation, leading to either relabelling or exclusion from the final solution.

The choice of the velocity model has the largest impact on the final location, and thus, on the uncertainty of the hypocentre. We evaluated each of the velocity models presented in Fig. 6 by relocating the 178 events with average magnitudes above 3 recorded after 1986. We selected this magnitude threshold and time period because we from this year had a more complete network, see Fig. 4(a)

Further, we apply quality criteria as proposed by Schweitzer *et al.* (2021) to assess the best-suited velocity model. We determine the best solution for a seismic event from a number of factors. A high-quality solution should have a large proportion of defining parameters (nd) relative to the total amount of observed parameters (nob). The number of defining parameters refers to the total number of parameters included in the final location calculation, such as phases, traveltime differences, slowness, and backazimuths. Observed parameters with extremely high residuals in the final location are excluded from the calculation, or their phase label is corrected. A solution that includes more observed parameters is generally indicative of higher quality.

Another important factor is the ratio of the number of defining traveltime residuals (ndtt) to the root-mean-square value (rms). A small rms indicates a good agreement between observed and predicted traveltimes, while a higher ndtt reflects the inclusion of more reliable data in the solution—a high ndtt combined with a small rms results in a higher quality solution.

The final quality metrics are based on a minimized L1 norm ($L1$) applied to all observed parameters encompassing backazimuths, traveltimes, slowness and traveltime differences, as well as a small source-time error (dt), and a small uncertainty ellipse (area). The L1 norm is calculated using the equation:

$$\frac{\sum \frac{|\text{res}|}{w}}{N}. \tag{1}$$

Here, res represents the residual for slowness, backazimuth, traveltimes, or traveltime differences, while the weight (w) used in the inversion corresponds to the assigned uncertainty. As noted earlier, we use a general uncertainty of 0.5 s for P-wave readings, which for P waves serves as the weight during the inversion process. Finally, the equation is normalized by the total number of residuals (N) included in the calculation. This process is performed separately for each parameter—backazimuth, slowness, and traveltime differences—and these individual L1 norms are then combined into a single overall L1 norm. For further details, we refer to Schweitzer (2018).

All these parameters are incorporated into the following equation from Schweitzer *et al.* (2021), which is used to determine the quality factor q:

$$q = \frac{\text{nd}}{\text{nob}} \cdot \frac{\text{ndtt}}{\text{rms}} \cdot \frac{1}{L_1 \cdot \text{d}t \cdot \text{area}}. \tag{2}$$

Note that the determined quality factor (q) is only valid for each individual event, and is not intended for comparison between events. For any given seismic event, the highest q value quantifies the most favourable solution.

In Fig. 7, we display the velocity models yielding the highest q for each of the 178 events. Unfortunately, no clear pattern emerges. In Table 2, we provide the fraction of events that obtain the highest q value if the respective velocity model is employed in the relocation process. The majority of the highest quality event locations are associated with the NNSN and FESCAN velocity models. In general, velocity models disregarding sediments tend to outperform models with slower velocities in the upper layers. This discrepancy may be caused by the seismic stations included in the event solution and their distribution. For instance, there is a clear predominance of seismic events occurring close to the Norwegian coastline with recording stations situated on bedrock.

Further, we examined the spread of earthquake locations when employing different models in the relocation process, focusing on three well-documented earthquakes. The first is the 1989 January 23 earthquake with a magnitude of M_s 5.1, studied by Hansen *et al.* (1989). The second is the 2001 May 7 earthquake with a magnitude of M_w 4.3, analysed by Ottemöller *et al.* (2005). The third is the 2017 June 30 earthquake with a magnitude of M_w 4.5 investigated by Jerkins *et al.* (2020).

Fig. 8 shows epicentral locations reported in these studies alongside those determined using the 10 different velocity models. Additionally, we present the uncertainty ellipse (in this case 95 per cent) for the velocity models associated with the highest q. The choice of velocity model significantly influences the hypocentral locations. Even the tightest clusters of locations exhibit a spread exceeding 10 km. The uncertainty ellipse provides a fit of observed data and traveltime tables and significantly underestimate the true location uncertainty caused by the lack of knowledge on the proper velocity model and the reduction of a 3-D velocity structure to a 1-D model. For all test events, four models stood out as outliers: BGS Dover, BGS Central NS, BGS South NS, and South Netherlands.

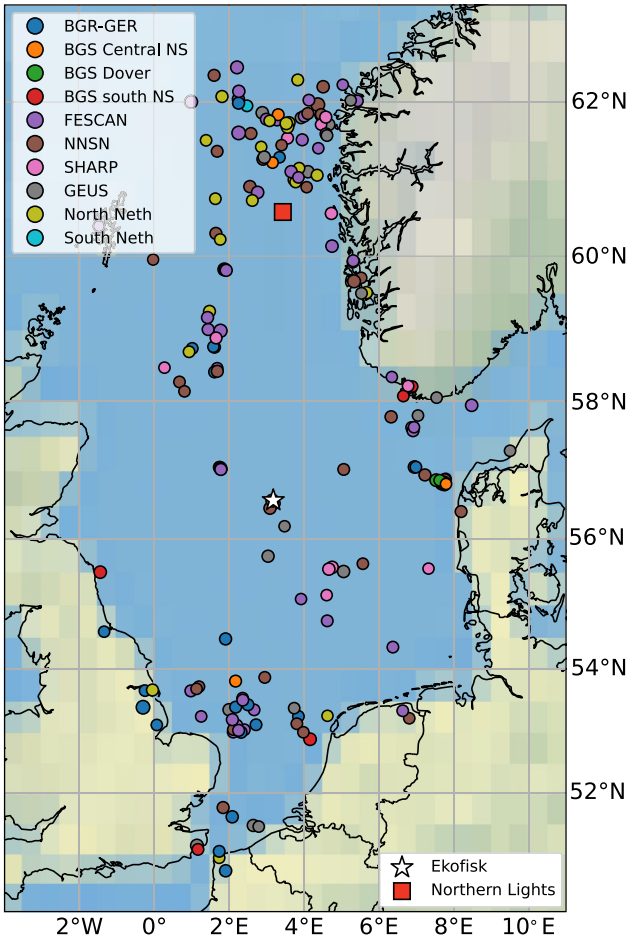

Figure 7. Map of the 178 test events, coloured by the velocity model which has the highest relocation quality factor q for that event. Refer to the legend for an explanation of colours.

Table 2. Number of events with the highest q (quality factor) for each velocity model among the 178 events depicted in Fig. 7. The right-hand column shows the average distance between event locations as computed employing the FESCAN model and locations derived using other velocity models.

Vel. model	Fraction of events with highest q for each model	Av. dist. FESCAN (km)
BGR-GER	20	9.9
BGS Central NS	5	24.5
BGS Dover	4	45.1
BGS South NS	5	32.2
FESCAN	48	–
NNSN	42	5.2
SHARP	11	14.7
GEUS	19	3.7
North Neth	22	9.8
South Neth	2	39.6

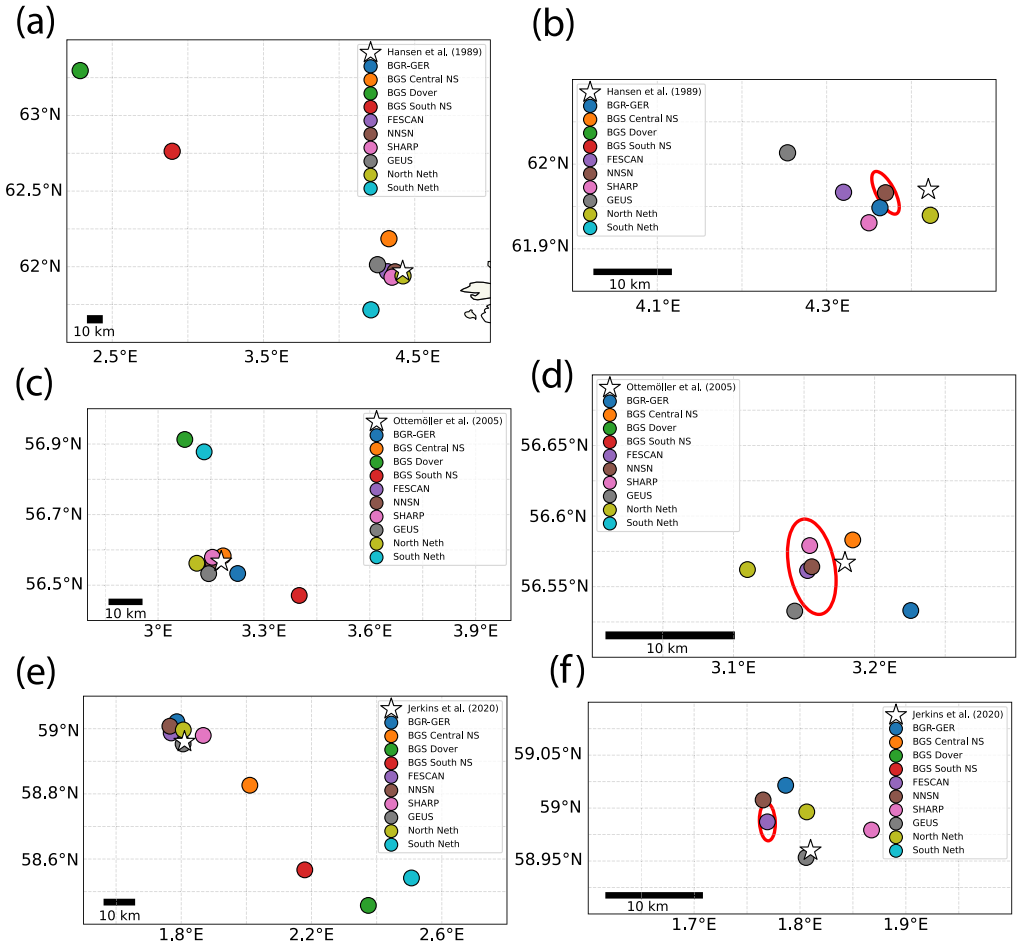

Figure 8. Velocity model test results: Panels (a) and (b) correspond to the 1989 January 23 M_s 5.1 event; (c) and (d) represent the 2001 May 7 M_w 4.3 event; and (e) and (f) show results for the 2017 June 30 M_w 4.5 event. Stars mark event locations as determined by Hansen *et al.* (1989), Ottemöller *et al.* (2005) and Jerkins *et al.* (2020), respectively. Panels (a), (c) and (e) present all computed event locations for each respective event, while panels (b), (d) and (f) provide a zoomed-in view of the main cluster of locations. The event location mark colour corresponds to the velocity model used to obtain it. The ellipse shows 95 per cent confidence ellipse associated with velocity model resulting in highest quality factor q.

We again note that these models are not designed for stations positioned on bedrock, and are tailored for a different geological setting with slower near surface velocities. As illustrated in Fig. 5, there is a sampling bias with a high proportion of seismic phase readings from the West coast of Norway, which likely introduce a bias when trying to identify the best-suited 1-D model. We decide on the use of the FESCAN model for further analysis as it exhibits the largest proportion of seismic events with the highest q (see Table 2). Subsequent computations were carried out using the criteria and input parameters described above.

Additionally, we extended HYPOSAT to include specific model uncertainties for local and regional seismic phases. This adjustment was prompted by the significant variation in event locations attributed to differences in velocity models. To address this, we assigned uncertainties based on the variability observed in traveltime curves for various seismic phases using the different velocity models in Fig. 6 over a distance of 1000 km. Specifically, we assigned an uncertainty of 4 s to the Pg phase, 3 s to the Pn phase, 8 s to the Sg phase, and 12 s to the Sn phase.

Fig. 9 presents event location statistics. For the majority of seismic events, the closest station is typically within a distance of less than one degree (≈111 km). However, for several of the seismic events in the central part of the North Sea, the distance is notably larger. Especially for events occurring before the year 1986, the distance to the closest station may exceed three degrees due to the sparse station network at that time. In addition, stations located within a radius of twice the event depth are required to get any sensitivity to depth, if no teleseismic depth phase readings are available (Havskov *et al.* 2012).

The average crustal thickness in the North Sea is about 30 km. Therefore, the fact that the distance to the closest station exceeds 0.5 deg (≈55 km) for 2924 events severely limits the ability to determine hypocentral depth.

Another significant challenge constraining earthquake locations is the large azimuthal gap. While 2202 events have azimuthal gaps smaller than 180°, only 157 events possess gaps of less than 90°, leading to significant uncertainties in the location estimates and inability to estimate focal mechanisms. Generally, more than 10 defining parameters (e.g. phase onset times, S-P difference, slowness and backazimuth) are available as input to the relocation process. The area of the spatial uncertainty ellipse is most often smaller than 200 km^2, and the RMS is often smaller than 1.5 s.

After relocation, we applied criteria based on Fig. 9 to filter significant outliers while retaining as many events as possible and

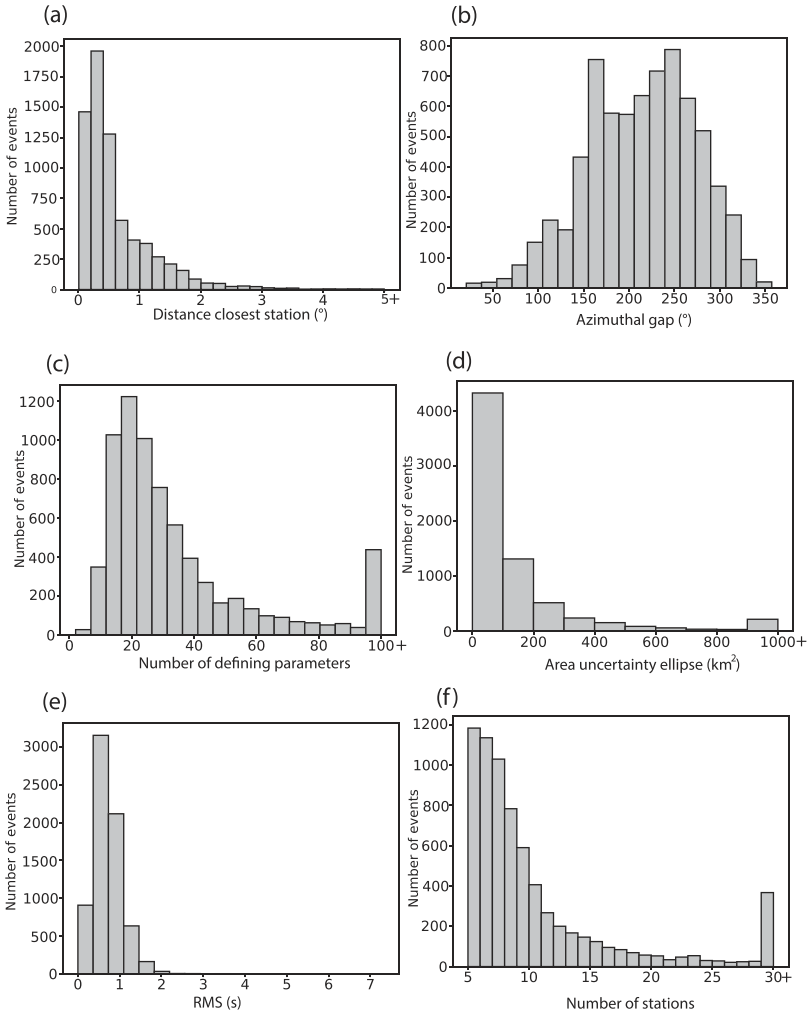

Figure 9. Event location statistics: (a) distance to the closest station, (b) azimuthal gap, (c) number of defining parameters, (d) area of the uncertainty ellipse, (e) root-mean-square of the residuals and (f) number of stations involved in relocation.

ensuring high-quality solutions. The chosen criteria include an average magnitude larger than 1, a distance to the closest station of less than 3°, a maximum azimuthal gap of less than 270°, an area of the error ellipse less than 400 km^2, the availability of more than 15 defining parameters, and an RMS of less or equal to 1.5 s.

A total of 4331 of the 7089 ($\approx$ 60 per cent) relocatable events meet these criteria. Fig. 10 compares the new locations to the original catalogue. The observed seismicity is slightly more tightly clustered for the relocations and often aligns along structures; for instance, the area between Norway and the Viking Graben shows fewer 'outliers' for the relocated catalogue. To better illustrate the improvements, Fig. 11 shows just the Viking Graben region. The seismicity for the relocated earthquakes is more tightly clustered than for the original catalogue. The arrow in Fig. 11 indicates a region where seismicity clustering is observed in the relocation. The enhancements are however less obvious as is the case for other data sets (for instance Raggiunti *et al.* 2023), possibly due to the unfavourable station distribution in the North Sea region, where there is often a significant distance to the nearest station and notable station gaps.

The depth distribution of the relocated seismic events is shown in Fig. 12. Although the depth estimates are poorly constrained, a concentration of events is observed between 0 and 15 km. However, we propose that the depth distribution is heavily influenced by the procedure and choice of velocity model—in this case, the FESCAN model—which could introduce artifacts into the depth distribution. Notably, the FESCAN model's upper crustal thickness is 16 km, aligning with the majority of events occurring at depths shallower than 15 km.

4 NEW UNCERTAINTY ESTIMATE AND LOCATIONS FROM UNCERTAINTY ELLIPSE ESTIMATES

As shown in Fig. 8, the uncertainty ellipses consistently underestimate the true location uncertainties due to lack of knowledge of the velocity model. Therefore, we refine the estimation of epicentre uncertainties using a pragmatic approach by examining the variability in earthquake locations caused by the usage of different 1D velocity models. To this end, we disregard locations derived from the BGS Dover, BGS South NS, BGS Central NS and South Netherlands models, as these models represented significant outliers in Fig. 8. Outliers in this context refer to seismic event locations that deviate significantly from the main cluster of event locations. These deviations are accompanied by a lower quality (q) for these events

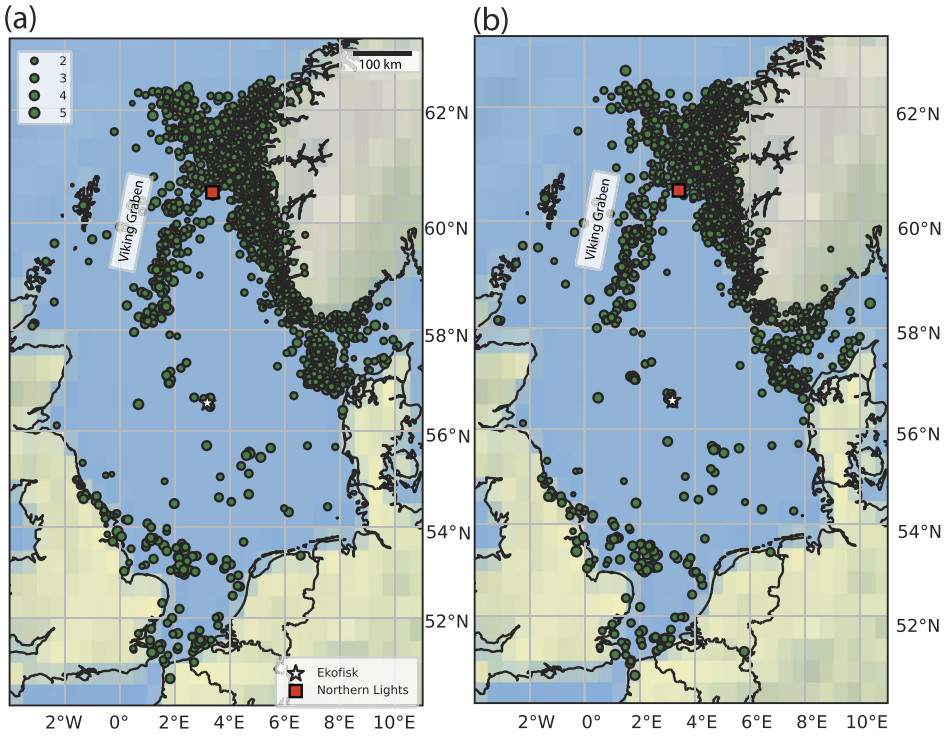

Figure 10. Out of the 7089 seismic events, 4331 meet the quality criteria. Here, we show the events before (a) and after (b) relocation, where we observe slightly improved spatial clustering, particularly between Denmark and Norway, along the Norwegian coastline, and within the Viking Graben.

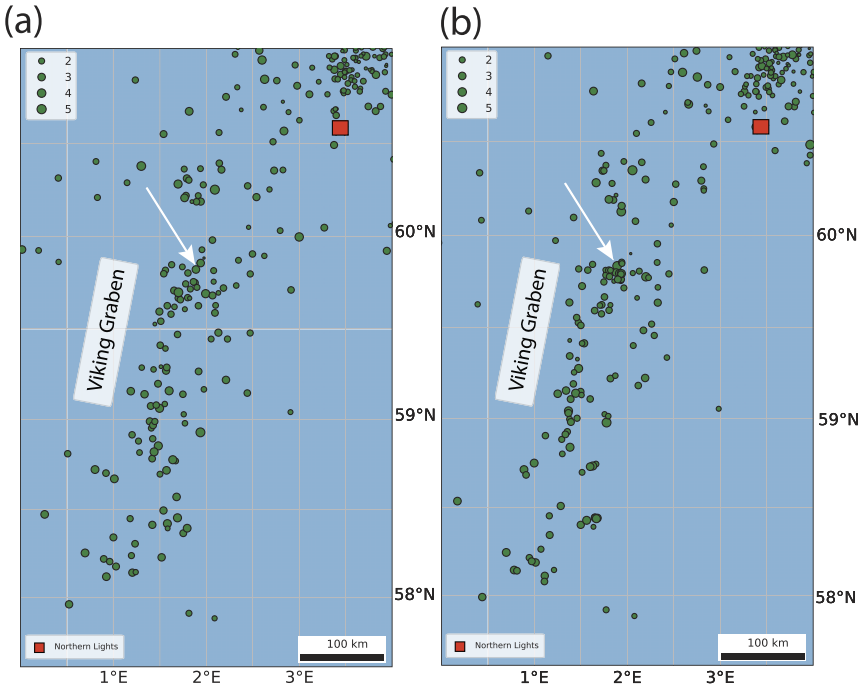

Figure 11. Close-up of the Viking Graben area for the same events as illustrated in Fig 10 before (a) and after relocation (b).The white arrow indicates a region where seismicity clustering is observed in the relocation.

compared to others, indicating reduced reliability in their location analysis. One possible cause for these deviations is that the closest stations for all these events are located in Norway, where sensors are placed on bedrock. Additionally, we consider seismic phases at regional distances of up to 10 deg. The outlier models appear to be more suitable for local-scale seismic events rather than regional-scale analysis.

Fig. 13(a) provides an example of this methodology. Specifically, we plot the 95 per cent uncertainty ellipse for each event location and determine a best-fitting ellipse that encompasses all individual

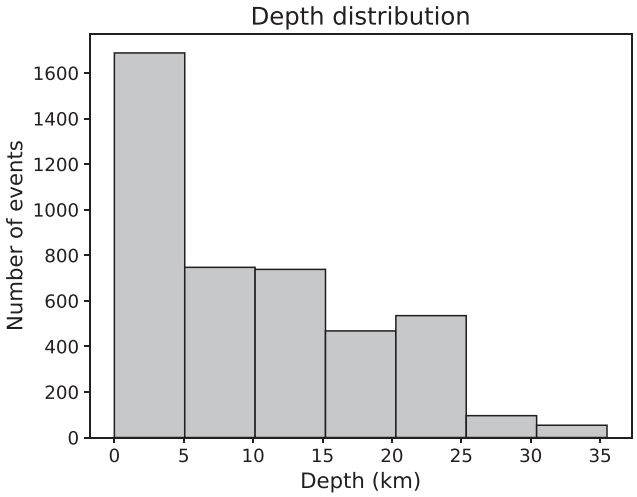

Figure 12. Depth distribution of relocated seismicity.

ellipses. Location uncertainty estimate are subsequently inferred from this best-fitting ellipse.

For the majority of seismic events, this methodology proved to be effective. However, in rare cases, a single solution deviated substantially from the bulk of locations, leading to a substantial overestimate of the uncertainty ellipse. To address this issue, we excluded the location furthest from the others whenever the ellipse major axis exceeded 70 km, and then estimated a new uncertainty ellipse. An example of this adjustment is presented in Fig. 13(b). In this case, using the SHARP model resulted in a clear outlier and the corresponding location was removed from the uncertainty ellipse estimate. This outlier exclusion was necessary in 370 out of the 4331 cases.

Fig. 13(c) presents a histogram of the new ellipse areas, revealing a significant increase in the sizes of the uncertainty ellipses compared to the original estimates (see Fig. 9d).The median area of the uncertainty ellipses for our relocations shown in Fig. 10 is 51.90 km^2. In contrast, the new uncertainty estimates yield a median ellipse area of 524.98 km^2, which is approximately 10 times larger. Although the overall distribution of the event relocations has not changed significantly, the uncertainty estimates for the event locations have improved considerably.

5 DISCUSSION

Determining earthquake locations in the North Sea has severe limitations. For instance, only 157 seismic events possess azimuthal gaps less than 90° and the event-to-station distances are often large, leading to less well-constrained hypocentre estimates. Given the current uncertainties for most seismic events, assigning specific earthquakes to individual faults in the North Sea is generally difficult. Accurate associations would require larger events, recorded by a high-quality seismic network with greater spatial coverage. Even then, significant interpretation would be needed, as highlighted by Jerkins *et al.* (2024). It is worth noting that fibre optic cables and permanent reservoir monitoring systems, already integrated into the current infrastructure of oil and gas reservoirs, could be utilized for routine passive seismic monitoring. Given their position offshore, they can help reduce the mentioned challenges by recording arrivals in offshore areas.

The application of existing offshore fibre optic cables was explored in various studies, including those by Williams *et al.* (2019), Bremaud *et al.* (2022) and Baird *et al.* (2025). Williams *et al.* (2019) employed a pre-existing submarine telecommunication cable off the coast of Belgium to investigate a variety of seismic sources, such as microseisms, local surface gravity waves and teleseismic earthquakes. Meanwhile, Bremaud *et al.* (2022) discuss the potential use of existing seabed cables for future CO_2 storage monitoring. Baird *et al.* (2025) specifically explored the use of an existing fibre-optic cable located just offshore of the United Kingdom, which is within the boundaries of our study region, for detecting and locating seismic events. Their work demonstrated that the fibre-optic cable alone can be effectively utilized to determine event locations. This highlights the potential of fibre-optic cables for detecting and locating seismic events in our study area. However, it is important to recognize the limitations of using fibre-optic cables, such as directional sensitivity, single-component data, poor constraints on the positioning of these cables, and unknown coupling conditions that affect signal quality, particularly magnitude estimates (Näsholm *et al.* 2022).

Additionally, Jerkins *et al.* (2023) demonstrated the potential of offshore permanent reservoir monitoring sensors, specifically those at the Grane oil field, to enhance the accuracy of seismic event locations in the North Sea by treating them as seismic arrays. Moreover, the use of onshore arrays was also proven to enhance location accuracy and reduce the detection threshold for seismic events. To this end, the Holsnøy array was installed on the west coast of Norway in 2020. Zarifi *et al.* (2023) showed that it not only detects more events than those recorded in existing catalogues, but also improves location accuracy by incorporating slowness and backazimuth estimates. However, the incorporation of industrial monitoring equipment such as offshore permanent reservoir monitoring sensors or existing seabed cables requires data sharing agreements that are not standard today.

Monitoring with ocean-bottom sensors offers significant potential. For example, a study on the Horda platform, focusing on the Northern Lights CCS site, demonstrated that these sensors can improve event locations (Shiddiqi *et al.* 2023). However, deploying ocean-bottom sensors, especially those capable of providing real-time data, is costly and poses challenges due to potential data quality issues caused by offshore noise.

Another challenge addressed in this study concerns velocity models. The 1-D models currently used by seismological agencies for event location are limited in capturing the geological variations across the region. Applying just a single 1-D model, as done here, is certainly not adequate. Additionally, often constant Vp/Vs ratios are applied, not considering Vp/Vs ratio changes with lithological units and depth (Brocher 2005). These shortcomings can significantly impact the hypocentre depth estimate. The above method of fitting an uncertainty ellipse aims to better represent the location uncertainty that result from these velocity model deficiencies.

While there are several smaller-scale 3-D velocity models available from oil and gas exploration, their maximum depth resolution is typically insufficient for regional earthquake locations. Furthermore, these models are not publicly available, and are therefore not available for scientific use. However, Crowder *et al.* (2021) developed a 3-D shear-wave velocity model for the North Sea using ambient noise tomography, reaching depths of around 30 km. This model displays variations in velocities across major geological formations, mapping features such as sedimentary basins and crustal thickness. The integration of this 3-D regional model, coupled with the future development of a similar *P*-wave model, has the potential to significantly enhance the accuracy of seismic event

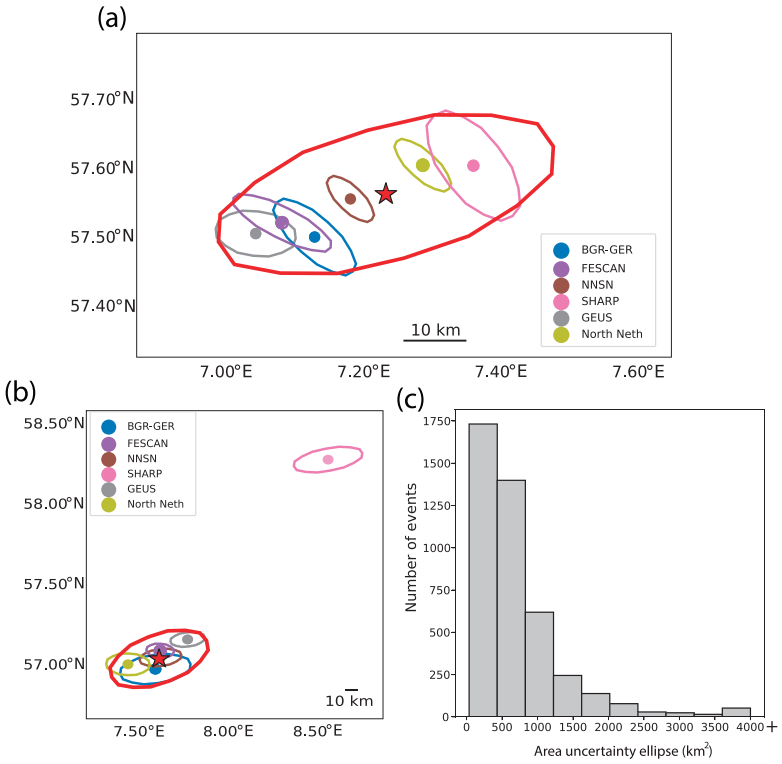

Figure 13. Pragmatic uncertainty estimates. (a) Locations derived from individual velocity models along with their corresponding 95 per cent confidence ellipses. New uncertainty estimate depicted by encompassing line, with the estimated centroid represented by a star. (b) Usage of SHARP model lead to significant outlier, which was therefore excluded from estimating uncertainty ellipse. (c) Histogram illustrating distribution of new uncertainty ellipses areas.

locations and reduce the biases associated with using 1-D models. It is worth noting that using noise-derived tomography (essentially surface wave tomography) directly for earthquake relocation would be highly challenging and may not work. However, this exercise is beyond the scope of this current work, necessitating a separate study. Also, implementing 3D models is often not possible in multiple location algorithms; for instance, this is the case for the HYPOSAT algorithm utilized here. A simpler alternative option is the application of station corrections. This would be especially beneficial for recent events detected with an already enhanced station network.

We observe that the location uncertainties are underestimated. Therefore, we re-evaluated the uncertainty ellipses using a pragmatic approach that accounts for the spread in earthquake locations. Considering the underestimation of earthquake location uncertainties, this issue poses challenges not only in the North Sea but also in regions with sparse monitoring networks or highly heterogeneous subsurface conditions. For instance, Turquet *et al.* (2019) demonstrated this problem in their study and developed a new grid search methodology to resolve this issue locating earthquakes in the Pyrenees.

Statistical methods and resampling techniques, such as the jackknife and bootstrap, offer potential to enhance uncertainty estimates in event locations and identify outlier stations. Oye & Roth (2003) applied the bootstrap method by repeating the inversion process multiple times, introducing random noise into the synthetic data for each iteration. For instance, ray tracing was employed to compute traveltime differences and polarization angles over a uniform grid within the observation volume, where the true event locations and corresponding data were pre-determined. This approach uses data variability to evaluate the reliability and robustness of the solution. They found that the final location is influenced by the specific noise values applied and the local gradients of the model parameters. Although the initial starting model was randomly selected, this choice did not affect the resulting location. In contrast, the jackknife method systematically removes one observation at a time to assess the impact of each data point on the overall estimate (Prieto *et al.* 2007). Although these methodologies are beyond the scope of this study, we recommend their application in future work.

Reporting realistic uncertainties associated with earthquake locations is crucial. Determining whether a small magnitude earthquake is induced or not is still often based largely on earthquake locations, although this only results in a qualitative, not a quantitative result. Quantitative discrimination is more difficult to assess (Dahm *et al.* 2010) and a probabilistic approach should be followed (Dahm *et al.* 2013) where possible. Currently, multiple oil and gas authorities in different countries operate with a traffic light system for oil and gas exploration, hydrofracturing and CO_2 storage projects. This system imposes regulations on when a project should be paused or shut down as a result of induced seismicity. In the UK, this system for hydraulic fracturing was particularly strict: if a M_L 0.5 earthquake was induced, operations must be paused until the earthquakes were reviewed by the regulator (Verdon & Bommer 2021). This low threshold was exceeded numerous times during each attempted hydraulic fracturing operation (Clarke *et al.* 2014; Kettlety *et al.* 2020, 2021). Given the existing onshore station network and 1-D velocity models, the location uncertainties are so significant that determining whether the event originated from the injection site and thus, might potentially be induced or triggered, would be impossible. It

would also impose significant uncertainty on the measurement of magnitude. Thus, this study highlights the need for additional or improved monitoring if similar traffic light regulations are applied to CO_2 storage.

In our relocation process, each event is considered individually, as is typical for regular matrix inversion location algorithms. Furthermore, applying relative event location codes such as Bayesloc (Myers *et al.* 2007, 2009) or the HypoDD algorithm (Waldhauser 2001), which consider multiple events simultaneously, can theoretically further reduce relative location uncertainties and improve event locations. Using HypoDD would require extensive waveform analysis and the station coverage would still influence the quality of the earthquake locations. For instance, Bai *et al.* (2006) demonstrated that achieving a hypocentral uncertainty of 1 km with a confidence level of 95 per cent using the HypoDD algorithm requires a station gap of less than $210^\circ \pm 15^\circ$, with 15 ± 2 stations located within 100 km of the epicentre. The station gap issue could for instance be reduced by extending the algorithm to incorporate backazimuth estimates as done by Dando *et al.* (2021).

During our analysis, we noticed that approximately half of the catalogued events are likely to be explosions (see Fig. 3). Considering reported event type metadata was used in the cleaning of the catalogue (Kettlety *et al.* 2024), it is clear that many of these likely explosions were unreported. It is crucial to accurately identify explosions in the North Sea in upcoming studies, particularly for risk and hazard assessments (though explosions would usually be excluded from hazard analyses due to their small size). Distinguishing earthquakes from explosions is typically performed by analysing signal characteristics. This has for instance been demonstrated in studies by Eggertsson *et al.* (2024) and Kortström *et al.* (2016). Kortström *et al.* (2016) implemented an automatic classification between earthquakes and explosions for seismic events in Finland using machine learning techniques. This algorithm classifies events based on the energy distribution of the recorded seismic signals, efficiently identifying 94 per cent of the man-made sources. Similarly, Eggertsson *et al.* (2024) applied machine learning techniques to seismic events in Sweden, successfully distinguishing between natural earthquakes and man-made sources. Adopting a similar machine-learning approach could minimize the number of explosions listed in our current and any future catalogues. Again, this requires extensive waveform analysis, while we here only focus on parameter data. Nonetheless, we suspect that a large number of these explosions originate from the west coast of mainland Norway, rather than being located in the North Sea.

This new relocation exercise led to seismic events being slightly more clustered than previously, resulting in more consistent seismicity patterns, along with providing uncertainty estimates, which are not routinely reported. By combining catalogues from different agencies, we included additional phase readings, thereby enhancing the quality of the earthquake locations. Thus, we recommend further collaboration between seismological agencies for better earthquake locations in the North Sea. Currently, as mentioned in the introduction, agencies use different methodologies, velocity models and quality criteria for their earthquake locations. It would be beneficial to agree on a common manner to relocate these earthquakes. The International Seismological Centre (2024) manually reviews and relocates events incorporating all phase readings delivered to them, but first, their bulletin is global and not concentrating on the North Sea and secondly, events are mainly reviewed for magnitudes of 3.5 and above.

6 CONCLUSION

We relocated a newly compiled catalogue of seismic events in the North Sea. The relocated and updated catalogue shows more tightly clustered seismicity aligned to structures. In addition, the relocation process added to our understanding of location uncertainties associated with earthquakes in the North Sea. Here, we show an average tenfold increase in the uncertainty estimates, giving a more realistic picture of the true uncertainties in the area, which is particularly important for offshore operations. Location accuracy and precision is limited by the lack of azimuthal station coverage as well as the large distances to the closest station, due to the fact that only onshore installations are permanently available. Further, the heterogeneous crustal structure of the North Sea cannot be represented by any 1-D velocity model. Thus, the application of a 3-D velocity model or at least a combination of several 1-D models is considered essential to reflect the large geological variations across the area.

ACKNOWLEDGMENTS

We would like to thank the institutes and the International Seismological Center (ISC) for their continuous provision of data and freely available products, which were essential to the success of this research.

This study was made possible by data from the following seismological networks: the German Regional Seismic Network (GR, Federal Institute for Geosciences and Natural Resources 1976), the Danish Seismological Network (DK, Geological Survey of Denmark and Greenland 2023), the GEOFON Seismic Network (GE, German Research Centre for Geosciences 1993), the Netherlands Seismic and Acoustic Network (NL, Royal Netherlands Meteorological Institute 1993), the NORSAR Station Network (NO, NORSAR (1971)), the Norwegian National Seismic Network (NS, Norwegian National Seismic Network 1982), the Magnus temporal network (2006–2008) (Z6, Weidle *et al.* 2010), the Belgian Seismic Network (BE, Royal Observatory of Belgium 1985), the Great Britain Seismograph Network (GB, British Geological Survey 1970) and the Kiel University Earthquake Monitoring Network (KQ, Christian Albrechts - Universitat zu Kiel (2017)).

We would also like to acknowledge Equinor (operating Grane, Oseberg, Snorre) and ConocoPhillips (operating Ekofisk) for providing data from their permanent reservoir monitoring networks to the Norwegian National Seismic Network. Additionally, we note that phases from the HNAR array (Equinor 2020), deployed to monitor the CCS storage site on the Horda platform, have been incorporated into the Norwegian bulletins since 2020.

We are also grateful to all collaborators in the SHARP project, including the Geological Survey of Denmark and Greenland (GEUS), the Royal Netherlands Meteorological Institute (KNMI), the British Geological Survey (BGS), NORSAR, British Petroleum (BP), Equinor, the Indian Institute of Technology Bombay (IIT Bombay), INEOS, the Norwegian Geotechnical Institute (NGI), the Norwegian University of Science and Technology (NTNU), the University of Oxford, Risktec, Rockfield, Shell, TU Delft, and Wintershall Dea.

Additionally, we would like to thank our colleagues and collaborators: Brian Baptie (BGS), P. Voss (GEUS), V. Maupin (University of Oslo), C. Bruland (NORSAR) and M. Kendall (University of Oxford).

The authors would also like to express their gratitude to the reviewers, Thomas Plenefisch and Tom Garth, for their valuable feedback. Additionally, they extend their thanks to the editors of Geophysical Journal International, for their support and guidance.

Finally, AEJ wishes to express her appreciation to the Norwegian National Seismic Network project, which has been the primary sponsor of her PhD research.

DATA AVAILABILITY

Data will be available at the end of the SHARP project in the ISF format via the ISC data repository: https://doi.org/10.31905/6TJZECEY

REFERENCES

Bai, L., Wu, Z., Zhang, T. & Kawasaki, I., 2006. The effect of distribution of stations upon location error: statistical tests based on the double-difference earthquake location algorithm and the bootstrap method, *Earth Planets Space,* **58,** e9–e12.

Baird, A.F., Morten, J.P., Oye, V. & Bjørnstad, S., 2025. Ocean space surveillance and real-time event characterization using distributed acoustic sensing on submarine networks, *Seismol. Res. Lett.,* 1–15, doi:10.1785/0220240360.

Bartholomew, I.D., Peters, J.M. & Powell, C.M., 1993. Regional structural evolution of the North Sea: oblique slip and the reactivation of basement lineaments, *Geol. Soc. Lond., Petrol. Geol. Conf. Ser.,* **4,** 1109–1122.

Bremaud, V., Rebel, E., Zamboni, E. & Sagary, C., 2022. DAS deployed at seabed for CO_2 storage monitoring, *Proc. 16th Greenhouse Gas Control Technologies Conf. (GHGT-16), 23–24 Oct 2022, Vol. 2022,* pp. 1–5, European Association of Geoscientists & Engineers

British Geological Survey -, BGS, 1970. Great Britain Seismograph Network. International Federation of Digital Seismograph Networks, Seismic Network, doi:10.7914/av8j-nc83.

Brocher, T.M., 2005. Empirical relations between elastic wave speeds and density in the Earth's crust, *Bull. seism. Soc. Am.,* **95**(6), 2081–2092.

Bungum, H., Alsaker, A., Kvamme, L.B. & Hansen, R.A., 1991. Seismicity and seismotectonics of Norway and nearby continental shelf areas, *J. Geophys. Res. Solid Earth,* **96**(B2), 2249–2265.

Bungum, H., Lindholm, C.D. & Dahle, A., 2003. Long-period ground-motions for large European earthquakes, 1905–1992, and comparisons with stochastic predictions, *J. Seismol.,* **7,** 377–396.

Bungum, H., Lindholm, C. & Faleide, J.I., 2005. Postglacial seismicity offshore mid-Norway with emphasis on spatio-temporal–magnitudal variations, *Mar. Petrol. Geol.,* **22**(1–2), 137–148.

Cappa, F. & Rutqvist, J., 2011. Modeling of coupled deformation and permeability evolution during fault reactivation induced by deep underground injection of CO_2, *Int. J. Greenh. Gas Control,* **5**(2), 336–346.

Cesca, S., Dahm, T., Juretzek, C. & Kühn, D., 2011. Rupture process of the 2001 May 7 Mw 4.3 Ekofisk induced earthquake, *Geophys. J. Int.,* **187**(1), 407–413.

Cheng, Y., Liu, W., Xu, T., Zhang, Y., Zhang, X., Xing, Y., Feng, B. & Xia, Y., 2023. Seismicity induced by geological CO_2 storage: a review, *Earth Sci. Rev.,* **239,** 104 369, doi:10.1016/j.earscirev.2023.104369.

Christian Albrechts - Universitat zu, Kiel, 2017. Kiel University earthquake monitoring, International Federation of Digital Seismograph Networks, doi:10.7914/SN/KQ.

Clarke, H., Eisner, L., Styles, P. & Turner, P., 2014. Felt seismicity associated with shale gas hydraulic fracturing: the first documented example in Europe, *Geophys. Res. Lett.,* **41**(23), 8308–8314.

Crowder, E., Rawlinson, N., Cornwell, D.G., Sammarco, C., Galetti, E. & Curtis, A., 2021. New insights into North Sea deep crustal structure and extension from transdimensional ambient noise tomography, *Geophys. J. Int.,* **224**(2), 1197–1210.

Dahm, T. *et al.*, 2010. How to discriminate induced, triggered and natural seismicity, in *Proc. Workshop Induced Seismicity: November 15–17, 2010, Hotel Hilton, Luxembourg; Grand-Duchy of Luxembourg,* pp. 69–76, Centre Européen de Géodynamique et de Séismologie.

Dahm, T. *et al.*, 2013. Recommendation for the discrimination of human-related and natural seismicity, *J. Seismol.,* **17,** 197–202.

Dando, B.D.E., Goertz-Allmann, B.P., Kühn, D., Langet, N., Dichiarante, A.M. & Oye, V., 2021. Relocating microseismicity from downhole monitoring of the Decatur CCS site using a modified double-difference algorithm, *Geophys. J. Int.,* **227**(2), 1094–1122.

Di Giacomo, D., Engdahl, E.R. & Storchak, D.A., 2018. The ISC-GEM earthquake catalogue (1904–2014): status after the extension project, *Earth Syst. Sci. Data,* **10**(4), 1877–1899.

Eggertsson, G., Lund, B., Roth, M. & Schmidt, P., 2024. Earthquake or blast? Classification of local-distance seismic events in Sweden using fully connected neural networks, *Geophys. J. Int.,* **236**(3), 1728–1742.

Engdahl, E.R., van der Hilst, R. & Buland, R., 1998. Global teleseismic earthquake relocation with improved travel times and procedures for depth determination, *Bull. seism. Soc. Am.,* **88**(3), 722–743.

Equinor (Norway), 2020. Equinor network is designed for passive monitoring of the CO2 storage sites in offshore Norway, International Federation of Digital Seismograph Networks, doi:10.7914/SN/QE.

Federal Institute for Geosciences and Natural Resources - BGR, 1976. *German Regional Seismic Network (GRSN),* Seismic Network, doi:10.25928/mbx6-hr74.

Furre, A.-K., Meneguolo, R., Ringrose, P. & Kassold, S., 2019. Building confidence in CCS: from Sleipner to the Northern Lights project, *First Break,* **37**(7), 81–87.

Furre, A.-K., Meneguolo, R., Pinturier, L. & Bakke, K., 2020. Planning deep subsurface CO_2 storage monitoring for the Norwegian full-scale CCS project, *First Break,* **38**(10), 55–60.

Garcia-Aristizabal, A., Danesi, S., Braun, T., Anselmi, M., Zaccarelli, L., Famiani, D. & Morelli, A., 2020. Epistemic uncertainties in local earthquake locations and implications for managing induced seismicity, *Bull. seism. Soc. Am.,* **110**(5), 2423–2440.

Geological Survey of Denmark and Greenland - GEUS, 2023. *National Seismic Network for the Kingdom of Denmark,* Geological Survey of Denmark and Greenland, Copenhagen, Denmark , doi:10.7914/nw3x-df02.

German Research Centre for Geosciences - GFZ, 1993. *GEOFON Seismic Network,* Seismic Network, doi:10.14470/TR560404.

Hansen, R.A., Bungum, H. & Alsaker, A., 1989. Three recent larger earthquakes offshore Norway, *Terra Nova,* **1**(3), 284–295.

Havskov, J., Bormann, P. & Schweitzer, J., 2012. Seismic source location, in *New Manual of Seismological Observatory Practice 2 (NMSOP-2),* pp. 1–36, Deutsches GeoForschungsZentrum GFZ.

Havskov, J. & Bungum, H., 1987. Source parameters for earthquakes in the northern North Sea, *Norsk Geologisk Tidsskr.,* **67,** 51–58.

Heidug, W., 2013. Methods to assess geologic CO2 storage capacity: status and best practice, *International Energy Agency Workshop Report,* Citeseer.

International Seismological Centre - ISC, 2024. doi:10.31905/d808b825.

International Seismograph Station Registry, 2024. *International Seismograph Station Registry (IR) - International Seismological Centre,* doi:10.31905/EL3FQQ40.

IPCC, Core Writing Team, Lee, H. & Romero, J., 2023. *Climate Change 2023: Synthesis Report. Contribution of Working Groups I, II and III to the Sixth Assessment Report of the Intergovernmental Panel on Climate Change,* pp. 35–115, IPCC, Geneva, Switzerland, doi:10.59327/IPCC/AR6-9789291691647.

Jerkins, A.E., Shiddiqi, H.A., Kværna, T., Gibbons, S.J., Schweitzer, J., Ottemöller, L. & Bungum, H., 2020. The 30 June 2017 North Sea earthquake: location, characteristics, and context, *Bull. seism. Soc. Am.,* **110**(2), 937–952.

Jerkins, A., Köhler, A. & Oye, V., 2023. On the potential of offshore sensors and array processing for improving seismic event detection and locations in the North Sea, *Geophys. J. Int.,* **233**(2), 1191–1212.

Jerkins, A.E., Oye, V., Alvizuri, C., Halpaap, F. & Kværna, T., 2024. The 21 March 2022 Tampen Spur Mw 5.1 Earthquake, North Sea: location, moment tensor and context, *Bull. seism. Soc. Am.,* **114**(2), 741–757.

Kettlety, T., Verdon, J.P., Werner, M.J. & Kendall, J.M., 2020. Stress transfer from opening hydraulic fractures controls the distribution of induced seismicity, *J. Geophys. Res. Solid Earth,* **125**(1), e2019JB018794, doi:10.1029/2019JB018794.

Kettlety, T., Verdon, J.P., Butcher, A., Hampson, M. & Craddock, L., 2021. High-resolution imaging of the ML 2.9 August 2019 earthquake in Lancashire, United Kingdom, induced by hydraulic fracturing during Preston New Road PNR-2 operations, *Seismol. Res. Lett.,* **92**(1), 151–169.

Kettlety, T., Martuganova, E., Kühn, D., Schweitzer, J., Weemstra, C., Baptie, B., Dahl-Jensen, T., Jerkins, A., Voss, P.H., Kendall, J.M. & Skurtveit, E., 2024. A unified earthquake catalogue for the North Sea to derisk European CCS operations, *First Break,* **42**(5), 31–36.

Kortström, J., Uski, M. & Tiira, T., 2016. Automatic classification of seismic events within a regional seismograph network, *Comput. Geosci.,* **87,** 22–30.

Laske, G., Masters, G., Ma, Z. & Pasyanos, M., 2013. Update on CRUST1.0—A 1-degree global model of Earth's crust, *Geophys. Res. Abstr.,* **15**(15), 2658.

Näsholm, S.P., Iranpour, K., Wuestefeld, A., Dando, B.D.E., Baird, A.F. & Oye, V., 2022. Array signal processing on distributed acoustic sensing data: directivity effects in slowness space, *J. Geophys. Res. Solid Earth,* **127**(2), e2021JB023587, doi:10.1029/2021JB023587.

Myers, S.C., Johannesson, G. & Hanley, W., 2007. A Bayesian hierarchical method for multiple-event seismic location, *Geophys. J. Int.,* **171**(3), 1049–1063.

Myers, S.C., Johannesson, G. & Hanley, W., 2009. Incorporation of probabilistic seismic phase labels into a Bayesian multiple-event seismic locator, *Geophys. J. Int.,* **177**(1), 193–204.

Mykkeltveit, S. & Ringdal, F., 1981. Phase identification and event location at regional distance using small-aperture array data, in *Identification of Seismic Sources—Earthquake or Underground Explosion: Proceedings of the NATO Advance Study Institute,* pp. 467–481, Springer.

NORSAR, 1971. *NORSAR Seismic Bulletins,* Seismic Network, doi:10.21348/b.0001.

Norwegian National Seismic Network - NNSN, 1982. *University of Bergen Seismic Network,* Seismic Network, doi:10.7914/SN/NS.

North Sea Transition Authority, 2024. *UKCS Storage Licences (WGS84),* https://opendata-nstauthority.hub.arcgis.com/datasets/NSTAUTHORITY::ukcs-carbon-storage-licences-wgs84/about (accessed 2024-10-24).

Ottemöller, L., Nielsen, H.H., Atakan, K., Braunmiller, J. & Havskov, J., 2005. The 7 May 2001 induced seismic event in the Ekofisk oil field, North Sea, *J. Geophys. Res. Solid Earth,* **110**(B10), doi:10.1029/2004JB003374.

Oye, V. & Roth, M., 2003. Automated seismic event location for hydrocarbon reservoirs, *Comput. Geosci.,* **29**(7), 851–863.

Prieto, G.A., Shearer, P.M., Vernon, F.L. & Kilb, D., 2007. Confidence intervals for earthquake source parameters, *Geophys. J. Int.,* **168**(3), 1227–1234.

Raggiunti, M., Keir, D., Pagli, C. & Lavayssière, A., 2023. Evidence of fluid induced earthquake swarms from high resolution earthquake relocation in the Main Ethiopian Rift, *Geochem. Geophys. Geosyst.,* **24**(4), e2022GC010765, doi:10.1029/2022GC010765.

Royal Netherlands Meteorological Institute - KNMI, 1993. *Netherlands Seismic and Acoustic Network,* Seismic Network, doi:10.21944/e970fd34-23b9-3411-b366-e4f72877d2c5.

Royal Observatory of Belgium - ROB, 1985. *Belgian Seismic Network,* Seismic Network, doi:10.7914/SN/BE.

Schweitzer, J., 2001. HYPOSAT—an enhanced routine to locate seismic events, *Pure Appl. Geophys.,* **158,** 277–289.

Schweitzer, J., 2018. User manual for HYPOSAT 6 and HYPOMOD 2, in *New Manual of Seismological Observatory Practice 2 (NMSOP-2),* pp. 1–38, Deutsches GeoForschungsZentrum GFZ.

Schweitzer, J., Paulsen, B., Antonovskaya, G.N., Fedorov, A.V., Konechnaya, Y.V., Asming, V.E. & Pirli, M., 2021. A 24-Yr-long seismic bulletin for the European Arctic, *Seismol. Res. Lett.,* **92**(5), 2758–2767.

Selby, N.D., Eshun, E., Patton, H.J. & Douglas, A., 2005. Unusual long-period Rayleigh wave radiation from a vertical dip-slip source: the 7 May 2001 North Sea earthquake, *J. Geophys. Res. Solid Earth,* **110**(B10), doi:10.1029/2005JB003721.

Shiddiqi, H.A., Ottemöller, L., Zarifi, Z., Bakke, R., Köhler, A., Jerkins, A. & Ringrose, P., 2023. Value of OBS seismicity monitoring to prepare for CO2 storage in the Hordaplatform, in *Proc. The 12th Trondheim Conference on CO2 Capture, Transport and Storage*.

Storchak, D.A., Schweitzer, J. & Bormann, P., 2003. The IASPEI standard seismic phase list, *Seismol. Res. Lett.,* **74**(6), 761–772.

Talwani, M. & Eldholm, O., 1977. Evolution of the Norwegian-Greenland sea, *Geol. Soc. Am. Bull.,* **88**(7), 969–999.

Turquet, A.L., Bodin, T., Arroucau, P., Sylvander, M. & Manchuel, K., 2019. Quantifying location uncertainties in seismicity catalogues: application to the Pyrenees, *J. Seismol.,* **23**(5), 1097–1113.

Verdon, J.P. & Bommer, J.J., 2021. Green, yellow, red, or out of the blue? An assessment of Traffic Light Schemes to mitigate the impact of hydraulic fracturing-induced seismicity, *J. Seismol.,* **25,** 301–326.

Waldhauser, F., 2001. hypoDD—a program to compute double-difference hypocenter locations Open-File Report 2001-113, U.S. Geol. Surv.

Weidle, C. *et al.*, 2010. MAGNUS—a seismological broadband experiment to resolve crustal and upper mantle structure beneath the Southern Scandes mountains in Norway, *Seismol. Res. Lett.,* **81**(1), 76–84.

Williams, E.F., Fernández-Ruiz, M.R., Magalhaes, R., Vanthillo, R., Zhan, Z., González-Herráez, M. & Martins, H.F., 2019. Distributed sensing of microseisms and teleseisms with submarine dark fibers, *Nat. Commun.,* **10**(1), 5778, doi:10.1038/s41467-019-13262-7.

Zarifi, Z. *et al.*, 2023. Background seismicity monitoring to prepare for large-scale CO_2 storage offshore Norway, *Seismol. Res. Lett.,* **94**(2A), 775–791.